ARTICLE

doi:10.1016/S1525-0016(02)00034-5

Free DNA Ends Are Essential for Concatemerization of Synthetic Double-Stranded Adeno-Associated Virus Vector Genomes Transfected into Mouse Hepatocytes *in Vivo*

Hiroyuki Nakai, Sally Fuess, Theresa A. Storm, Leonard A. Meuse, and Mark A. Kay*

Departments of Pediatrics and Genetics, Stanford University School of Medicine, Stanford, California 94305

**To whom correspondence and reprint requests should be addressed. Fax: (650) 498-6540. E-mail: markay@stanford.edu.*

Recombinant adeno-associated virus (rAAV) vectors stably transduce hepatocytes *in vivo*. In hepatocyte nuclei, the incoming single-stranded (ss) vector genomes are converted into various forms of double-stranded (ds) genomes including extrachromosomal linear and circular monomers and concatemers, and a small portion of the vector genomes integrate into chromosomes. The mechanism of genome conversion is not well understood. In the present study, we analyzed the role of inverted terminal repeat (ITR) sequences of ds circular or linear rAAV vector intermediates in concatemerization. We synthesized supercoiled ds circular monomers with a double-D ITR (DDITR) (C+), and ds linear monomers with an ITR at each end (L+), and their control molecules, C− and L− , which lack the ITR-derived sequences, and transfected mouse hepatocytes with these molecules *in vivo* to assess their capacity for concatemerization. The transfected L+ or L−, but not C+ or C− molecules, concatemerized *in vivo* irrespective of the presence or absence of the ITRs. In addition, our results suggested that transfected C+ or C− species were not efficient substrates for integration. Based on these observations, we propose a model whereby ds linear molecules with free DNA ends, but not circular molecules, play an important role in rAAV vector genome concatemerization.

Key Words: adeno-associated virus, gene therapy, mouse, liver, inverted terminal repeat, recombination, integration, double-stranded DNA, naked DNA, Factor IX

INTRODUCTION

Adeno-associated virus (AAV) is a nonpathogenic replication-defective human parvovirus with a single-stranded (ss) DNA genome of ~ 4.7 kb. The recombinant AAV (rAAV) vector is a promising vehicle for delivery of transgenes to various tissues because it can direct persistent transgene expression *in vivo*. Recently a series of new rAAV technologies have been established, including the use of two complementary rAAV vectors to increase the limited packaging capacity of rAAV [1–3], modification of capsid proteins for retargeting [4], development of rAAV vectors based on serotypes other than type 2 [5–7], and self-complementary double-stranded (ds) rAAV vectors [8] to enhance transgene expression. All of these developments have the potential to expand the utility of rAAV vectors. Gene transfer clinical trials using rAAV vectors are currently underway for the treatment of cystic fibrosis, hemophilia B, and limb girdle muscular dystrophy [9–11].

Despite the recent advances in the practical use of rAAV vectors for *in vivo* gene therapy, the mechanism of *in vivo* transduction has not been fully elucidated. We and others have been engaged in unraveling these mechanisms of rAAV transduction in hepatocytes *in vivo,* and have demonstrated that (1) following *in vivo* administration of rAAV vectors, all the hepatocytes take up ss rAAV vector genomes but only ~ 5% cells can be stably transduced irrespective of the status of cell cycling [12,13]; (2) the majority of stably transduced vector genomes are ds genomes formed by annealing of complementary plus and minus ss vector genomes [14]; (3) the stably transduced rAAV genomes in hepatocytes exist as supercoiled ds circular monomers, and large circular and linear concatemers, with the occasional presence of ds linear monomers [12,14,15]; (4) concatemerization occurs through intermolecular recombination of input genomes, not by a rolling-circle amplification, and the linking orientation is random [14]; (5) a large proportion of these ds genomes,

Copyright © The American Society of Gene Therapy
1525-0016/03 $30.00

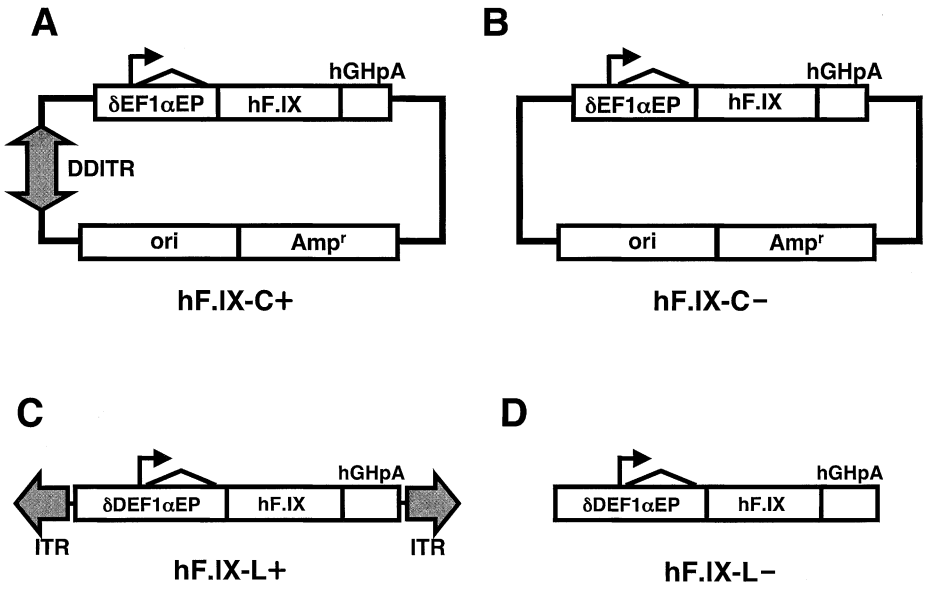

FIG. 1. Maps of ds circular and linear DNAs. (A, B) Supercoiled ds circular plasmids with or without a DDITR (hF.IX-C+ or hF.IX-C−, respectively). (C, D) Ds linear DNA with or without ITRs (hF.IX-L+ or hF.IX-L−, respectively). (C) and (D) are blunt-ended *Pvu*II-*Pvu*II ds linear fragments from pVm4.1eδD-hF.IX and pBSδD-hF.IX, respectively. ITR, 130-bp AAV inverted terminal repeat; DDITR, 165-bp double-D ITR; δEF1αEP and δDEF1αEP, truncated versions of the human elongation factor 1α gene enhancer-promoter (EF1αEP) that have the same enhancer-promoter activity [14,16,31] as the full-length form [30]; hF.IX, human coagulation Factor IX cDNA; hGHpA, the human growth hormone gene polyadenylation signal; ori, plasmid origin of replication from pUC; Amp^r, the ampicillin resistance gene.

including large concatemers, reside as extrachromosomal genomes [15]; (6) only a small proportion of rAAV genomes integrate into chromosomes [12,15–17]. To elucidate the mechanisms involved in rAAV transduction *in vivo,* the process of rAAV vector genome concatemerization and integration must be determined.

The inverted terminal repeat (ITR) of AAV is a T-shaped hairpin structure consisting of four regions: A, B, C, and D. The ITR sequence is essential for AAV genome replication, integration, and packaging into viral particles. A recent study by Yang *et al*. suggested that concatemerization of rAAV vector genomes occurred through the ITR sequences in ds circular genomes [18]. However, the importance of the ITR sequence in genome concatemerization has not been fully established. As a first step toward elucidating the mechanisms of rAAV vector genome conversion, we synthesized ds circular DNA molecules with a DDITR [19,20], and ds linear rAAV vector genomes, then introduced them into mouse hepatocytes *in vivo* by a hydrodynamics-based transfection technique, and analyzed the transfected livers for vector genome concatemerization by Southern blot. Double-stranded circular genomes with a DDITR and ds linear genomes with an ITR at each end are analogous to ds circular and linear rAAV genomes observed in rAAV vector-transduced mouse hepatocytes *in vivo* [14,19]. While it cannot be fully established whether hydrodynamics-based transfection mimics rAAV vector transduction, the synthetic ds circular and linear rAAV vector genomes used in the present study demonstrated that the DDITR sequences contained within transfected ds circular DNA molecules did not mediate concatemerization, while ds linear genomes were efficiently converted to concatemers irrespective of the presence or absence of ITR sequences. The structures generated by injection of these DNAs were similar to those formed in rAAV vector transduction. This suggested that free DNA ends present on ds rAAV vector genomes, rather than the ITR sequences themselves, might be essential for vector genome concatemerization in bona fide rAAV vector-mediated hepatocyte transduction *in vivo*.

RESULTS

Tail Vein Injection of Circular Human Factor IX (hF.IX)-Expressing Vectors, With or Without the DDITR (hF.IX-C+ or hF.IX-C−), Results in Persistent and Therapeutic Levels of Human F.IX in Mouse Plasma

The synthetic ds circular rAAV genome, hF.IX-C+, and its control, hF.IX-C−, are shown in Figure 1. All the molecules used in this study were monomer genomes purified by agarose gel fractionation to remove concatenated molecules (Fig. 2). To study the molecular fate of ds circular DNA with or without the DDITR in mouse hepatocytes *in vivo,* we transfected 25 μg of hF.IX-C+ (group 1, $n = 37$) or hF.IX-C− (group 2, $n = 25$) into the livers of C57BL/6 mice by tail vein injection. Irrespective of the presence or absence of the DDITR, injection of hF.IX-C+ or hF.IX-C− molecules resulted in long-term therapeutic levels of human F.IX in mouse plasma (Fig. 3). The mechanism underlying the persistent expression was unclear, but this result indicated that the presence of the DDITR did not have any effect on transgene expression *in vivo,* in contrast to a previous observation *in vitro* [21].

Copyright © The American Society of Gene Therapy

doi:10.1016/S1525-0016(02)00034-5

DDITR in Transfected ds Circular Genomes Does Not Mediate Efficient Integration in Hepatocytes *in Vivo*

We have earlier shown that surgical partial hepatectomy is a powerful tool for distinguishing between transgene expression from extrachromosomal vector genomes and integrated vector genomes in hepatocytes [15]. Following a partial hepatectomy, extrachromosomal transgene expression was lost while expression from integrated vector genomes remained stable [15]. To investigate the ability of ds circular genomes with a DDITR to integrate into chromosomes *in vivo,* we performed a partial hepatectomy at day 1 ($n = 3$ each in groups 1 and 2), day 4 ($n = 5$, group 1; and $n = 3$, group 2), week 1 ($n = 5$ and $n = 3$), week 3 ($n = 3$, each group), and week 20 ($n = 6$ and $n = 3$) after vector injection. Human F.IX levels were measured at the time of, 1 week, and 3 weeks after hepatectomy. As shown in Figure 4, human F.IX expression from either hF.IX-C+ or hF.IX-C− was substantially diminished after hepatectomy, together with a substantial loss of vector genomes (Fig. 5A), suggesting no appreciable amount of integration of these molecules in hepatocytes.

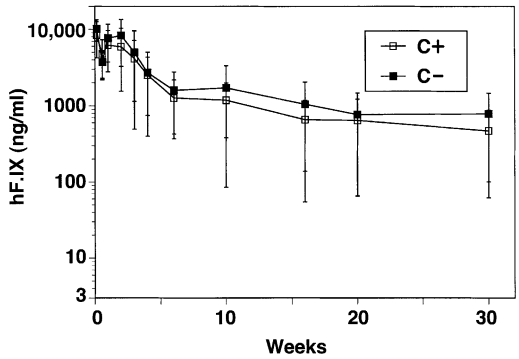

FIG. 3. Human F.IX levels in mouse plasma after tail vein injection of supercoiled monomeric ds circular molecules, hF.IX-C+ or hF.IX-C−. Plasma human F.IX levels in mice injected with 25 μg of gel-purified monomeric hF.IX-C+ or hF.IX-C− through the tail vein. Initially, 37 (hF.IX-C+) and 25 (hF.IX-C−) mice were injected, but some of the mice were partially hepatectomized and killed at several time points (see Fig. 4 and Results). Vertical bars indicate standard deviations.

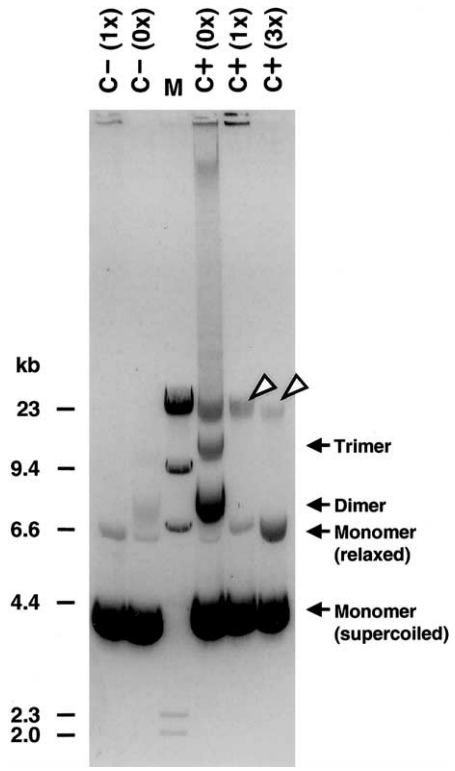

FIG. 2. Concatenation of hF.IX-C+ molecules in *E. coli.* We separated 2 μg aliquots of unfractionated and agarose gel-fractionated hF.IX-C+ or hF.IX-C− plasmid DNA preparations that had been purified by CsCl gradient on a 0.8% agarose gel, and stained them with ethidium bromide. Considerable concatenation was observed in the unfractionated hF.IX-C+ preparation (C+, 0×), but not in the hF.IX-C− preparation (C−, 0×). Open arrowheads indicate aggregation of monomeric hF.IX-C+ molecules migrating at a high-molecular-weight position that could not be removed by one cycle (C+, 1×) or three cycles (C+, 3×) of gel fractionation. The size marker (M) is *Hin*dIII-digested λ-DNA.

To analyze further the proportion of integrated versus extrachromosomal vector genomes, we conducted a *Dpn*I resistance assay based on differential methylation of DNA derived from bacterial plasmids and from mammals. Bacterial-derived methylated DNA loses methylation and becomes resistant to *Dpn*I digestion after DNA replication, such as that induced by hepatocellular regeneration with a surgical partial hepatectomy. After liver regeneration, *Dpn*I-resistant genomes represent integrated vector genomes unless the vector DNA replicates as episomes. The results of the *Dpn*I resistance assay in mice injected with hF.IX-C+ or hF.IX-C− molecules showed no detectable genome replication before and after partial hepatectomy performed 1 day and 20 weeks after injection (Figs. 5B and 5C). These results taken together indicate that, at the sensitivity level of the assay, hF.IX-C+ or hF.IX-C− molecules were not integrated into chromosomal DNA *in vivo.*

DDITR in Transfected ds Circular Genomes Does Not Mediate Concatemerization in Hepatocytes *in Vivo*

To address directly the question whether the DDITR sequence mediates concatemerization of circular vector genomes, we introduced synthetic ds circular rAAV vector genomes with DDITR into hepatocytes *in vivo* and investigated intermolecular recombination or joining by Southern blot analysis at different time points after vector injection. In the mice injected with hF.IX-C+ or hF.IX-C− molecules, total genomic DNA was extracted from livers harvested at the time of partial hepatectomy performed at days 1 and 4, and weeks 1, 3, and 20 after vector injection, and the molecular forms of hF.IX-C+ or hF.IX-C− molecules were determined. Because rAAV vector genome concatemerization occurs through intermolecular

Copyright © The American Society of Gene Therapy

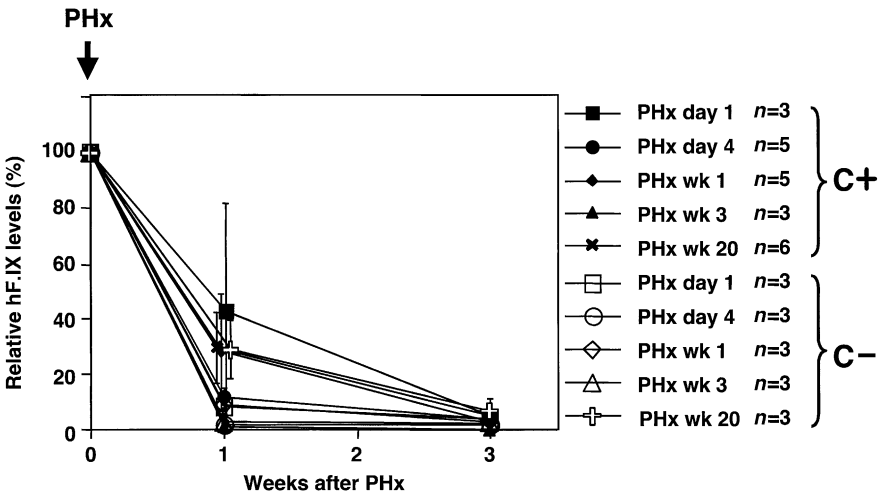

FIG. 4. Human F.IX levels after partial hepatectomy of mice injected with hF.IX-C+ or hF.IX-C− molecules. A two-thirds surgical partial hepatectomy (PHx) was performed on mice injected with 25 μg of monomeric hF.IX-C+ or hF.IX-C− at days 1 and 4, and weeks 1, 3, and 20 after injection. The y-axis represents the percentage of human F.IX levels relative to the levels at the time of PHx. Vertical bars indicate standard errors. Large standard errors observed 1 week after PHx were due to transient increases of human F.IX levels after PHx, before a substantial drop.

recombination or joining in mouse livers [14], it is essential that a hepatocyte acquires at least two vector molecules during DNA transfection. Southern blot analysis of liver DNA extracted 1 day after vector injection revealed that on average each hepatocyte had 15.2 ± 3.4 ds vector genomes (mean ± SD, $n = 4$, or $n = 2$ each from groups 1 and 2, data not shown), sufficient numbers in theory to allow vector genomes to concatemerize. However, there was no high-molecular-weight signal after restriction digestion with an enzyme that does not cleave within the vector (*Kpn*I), or from undigested DNA, at any of the time points examined (Fig. 5D, and data not shown), suggesting absence of large concatemers.

The relaxed ds circular monomers and supercoiled ds circular dimers have similar electrophoretic mobility on agarose gels (see Fig. 2), making them more difficult to differentiate. However, the majority of molecules that migrate at a position higher than ds linear molecules (RdsCM position in Fig. 5D) should represent relaxed circular monomers, not supercoiled circular dimers, based on the following observations: First, the intensity of the bands migrating at the RdsCM position was faint when undigested DNA was analyzed, but increased when incubated with a non-cutter enzyme. In addition, the same digestion resulted in a decrease in the intensity of supercoiled ds circular monomers (Fig. 5D). The incubation of the sample DNA with a non-cutter enzyme may result in nonspecific nicks in DNA, converting supercoiled circular monomers into relaxed circular forms. If the bands at the RdsCM position had represented supercoiled ds circular dimers, nicking of the DNA should result in a decrease in the band intensity. Second, partial digestion of the DNA with a single-cutter enzyme did not decrease the intensity of the bands at the RdsCM position although there was a substantial increase and decrease in the intensity of bands representing linear and supercoiled circular monomer forms, respectively (Fig. 5E). This suggests that the bands at the RdsCM position represent relaxed supercoiled monomers and not supercoiled circular dimers. Relaxed circular monomers can be converted into ds linear forms with single-cutter enzyme digestion and can be converted from supercoiled circular monomers with nonspecific nicking. Third, because supercoiled circular monomers normally contain DNA populations with varying degrees of relaxed forms, relaxed circular dimers should be observed if supercoiled circular dimers were present. However, there were no bands in the DNA samples indicative of relaxed circular dimers. Taken together, these results demonstrate that transfected hF.IX-C+ or hF.IX-C− did not dimerize or concatemerize in hepatocytes *in vivo*.

Double-Stranded Linear Genomes Efficiently Concatemerize in Hepatocytes *in Vivo*

The studies above suggested that transfected ds circular genomes with a DDITR did not serve as substrates for concatemerization. Thus, we focused on ds linear molecules as substrates for further recombination. We produced synthetic ds linear rAAV genomes (hF.IX-L+), and its control that lacked ITRs (hF.IX-L−) (Fig. 1). These ds linear vector genomes carried essentially the same EF1α enhancer-promoter-driven human F.IX expression cassette (Fig. 1) as hF.IX-C+ and C−. We injected 11 mice through the tail vein with either 23 μg or 91 μg of hF.IX-L+, 7 mice with 22 μg of hF.IX-L−, and 14 mice with either 25 μg or 100 μg of hF.IX-C+. Each dose of the vector was determined from the molecular weight of the vector such that animals would receive the same number of (1×) or four times more (4×) DNA molecules. In all cases, persistent therapeutic levels of human F.IX expression were achieved, and there was no substantial difference in human F.IX levels between the 1× and 4× doses. The hF.IX levels 6 weeks after injection were 9486 ± 1664 ng/ml in mice injected with hF.IX-L+, 4172 ± 335 ng/ml in mice injected with hF.IX- L−, and 3295 ± 988 ng/ml in

Copyright © The American Society of Gene Therapy

doi:10.1016/S1525-0016(02)00034-5

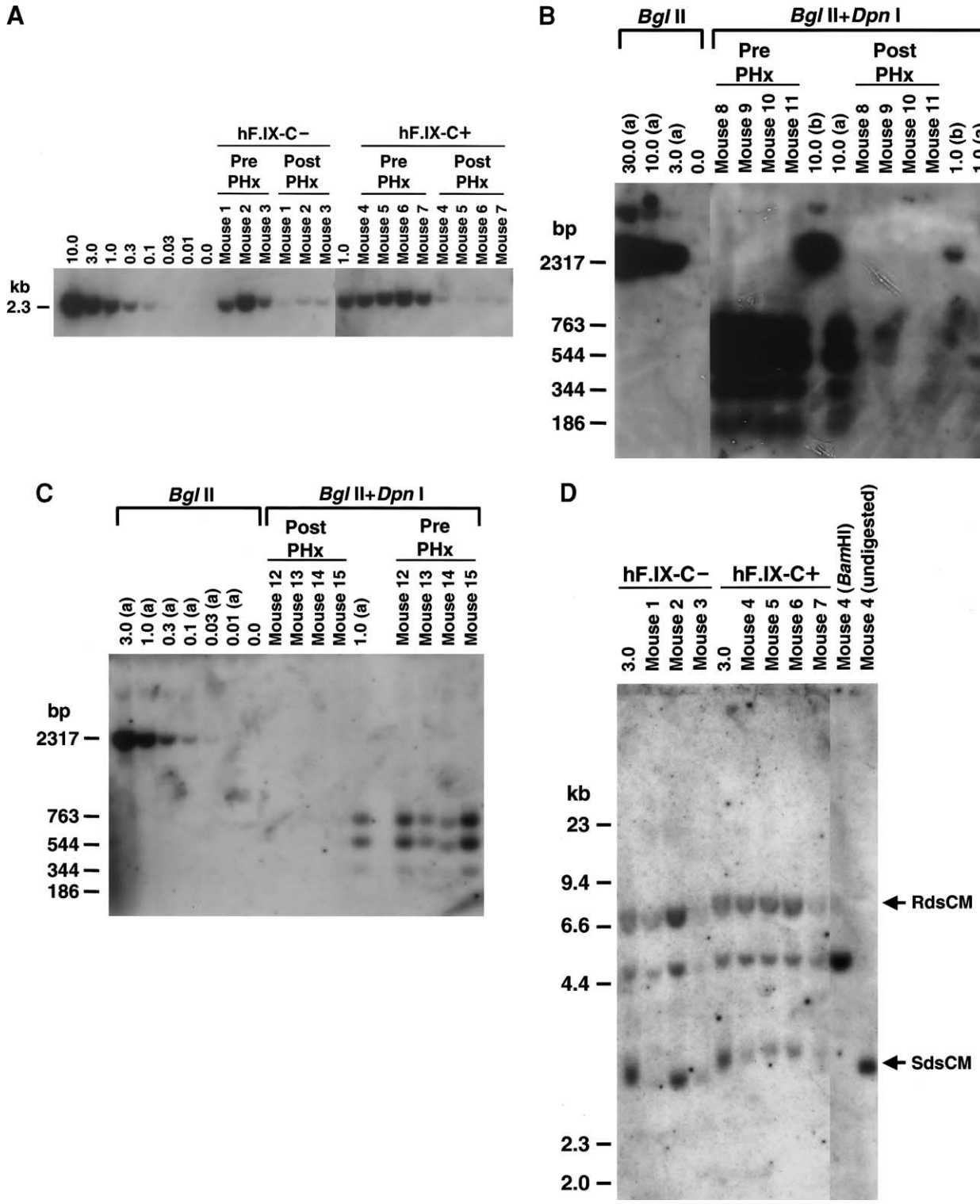

Copyright © The American Society of Gene Therapy

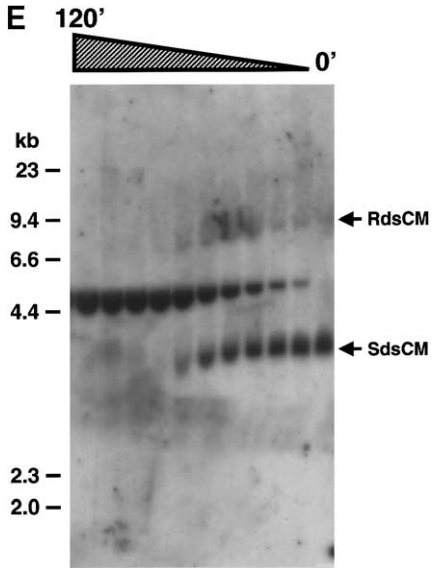

FIG. 5. Southern blot analysis of vector genomes in mouse livers transfected with hF.IX-C+ or hF.IX-C− molecules. (A) Analysis of copy numbers of transfected DNA molecules before and after partial hepatectomy (PHx). C57BL/6 mice were injected with 25 μg of monomeric hF.IX-C− (mice 1–3) or hF.IX-C+ (mice 4–7), and underwent a two-thirds partial hepatectomy 20 weeks after injection. Total DNA was extracted from livers harvested at the time of, and 3 weeks after hepatectomy, and 20 μg of each DNA sample was subjected to Southern blot analysis with *Bgl*II that cuts the vector genomes twice within the EF1α-hF.IX expression cassette. The vector genome copy number standards (0.0 to 10.0 copies per diploid genomic equivalent) were 20 μg of naive mouse total liver DNA mixed with the appropriate amount of agarose gel-fractionated monomeric hF.IX-C+. (B, C) Analysis of replicated vector genomes before and 3 weeks after PHx, performed (B) a day or (C) 20 weeks after injection. The numbers 0.0–30.0 indicate vector genome copy number standards based on hF.IX-C− (a) or a *Dpn*I-resistant plasmid, pV4.1e-hF.IX.dam- (b). Mice 8, 9, 12, and 13 were injected with hF.IX-C+, whereas mice 10, 11, 14, and 15 received hF.IX-C−. *Dpn*I-resistant replicated vector genomes migrated at 2317 bp (see lanes 10.0 (b) and 1.0 (b) in panel B), whereas *Dpn*I-sensitive unreplicated genomes were digested into smaller fragments of 763, 544, 344, and 186 bp. No *Dpn*I-resistant genomes were observed in mouse samples. (D) Analysis of vector genomes by Southern blot with a non-cutter enzyme *Kpn*I. The 3.0 copy-per-cell standards were based on monomeric hF.IX-C− or hF.IX-C+. The two lanes farthest to the right represent undigested and *Bam*HI-digested liver DNA from mouse 4. *Bam*HI cleaves the vector genome once between the promoter and the hF.IX cDNA. The signals from supercoiled ds circular monomers (SdsCM) and relaxed ds circular monomers (RdsCM) are indicated by arrows. Note that there are no high-molecular-weight signals, demonstrating no concatemerization of the vector genomes. (E) Partial digestion of the liver DNA with a single-cutter enzyme, *Bam*HI. Samples of the liver DNA from mouse 5 (20 μg) were undigested or digested with 8 units of *Bam*HI for 2, 5, 10, 15, 20, 30, 40, 50, 60, and 120 minutes, and subjected to Southern blot analysis. A *Bgl*II hF.IX probe [14] was used for all the blots.

mice injected with hF.IX-C+ (means ± SE). In this experiment, hF.IX-L+ resulted in higher human F.IX levels than hF.IX-L− (Student's *t*-test, $P = 0.016$); however, in two other independent experiments, the difference in human F.IX expression between hF.IX-L+ and hF.IX-L− did not reach statistical significance (data not shown).

The total numbers of hF.IX-L+, hF.IX-L−, and hF.IX-C+ vector genomes found in the liver 6 weeks after injection as determined by quantitative Southern blot analysis were 13.9 ± 5.4, 7.6 ± 4.5, and 5.8 ± 3.6 copies per diploid genomic equivalent ($n = 4$ each, means ± SD), respectively (data not shown). In contrast to the results with the hF.IX-C+ molecule, hF.IX-L+ and hF.IX-L− molecules efficiently concatemerized *in vivo,* forming large concatemers (Fig. 6A). Southern blot analysis using restriction enzymes that cut near the 5′ (*Sac*I) or 3′ (*Hin*dIII) ends of the linear vector genomes (see Fig. 6C) revealed the presence of equal amounts of head-to-tail, head-to-head, and tail-to-tail concatemers (Figs. 6A and 6B), demonstrating that the linking orientation was random as seen in rAAV vector concatemers *in vivo* [14]. It should be noted that the molecular fate of transfected hF.IX-L+ and hF.IX-L− molecules appeared to be similar to that of rAAV vector genomes in rAAV vector-transduced mouse liver—that is, conversion into head-to-tail, head-to-head, and tail-to-tail concatemers, supercoiled ds circular monomers, and ds linear monomers [14,16]. Taken together, these results showed that free DNA ends, rather than the ITR sequence, present in ds vector genomes have an important function in concatemerization *in vivo,* and suggested that the ITR sequence is dispensable for concatemerization as earlier reported [22].

DISCUSSION

The present study was designed to further our understanding of the mechanisms of rAAV genome conversion *in vivo*. The ability to transfect hepatocytes with naked DNA *in vivo* allowed us to investigate directly the fate of different forms of transfected ds rAAV vector genomes. Our results demonstrate that ds linear vector genomes, but not circular vector forms, represent molecular intermediates for concatemerization *in vivo*. Furthermore, our data demonstrate that the presence of free DNA ends, not the ITR sequence itself, is essential for efficient concatemerization of dsDNA molecules transfected in hepatocytes *in vivo*.

Our findings are not consistent with the findings by Yang *et al.* that supercoiled ds circular rAAV vector genomes are intermediates for concatemerization [18]. This hypothesis was based on an observation that co-injection of mouse muscle with a vector expressing alkaline phosphatase (AP) together with a vector expressing enhanced green fluorescent protein (EGFP) resulted in a time-dependent increase in the abundance of circular genomes consisting of the genes encoding both AP and EGFP, and not based on direct studies demonstrating that circular molecules, not linear molecules, recombined and formed concatemers. It is possible that the mechanisms of rAAV vector genome concatemerization are different in muscle and liver, or cellular proteins that mediate intermolecular recombination or joining of circular molecules are particularly induced by rAAV vector transduction, not by naked

Copyright © The American Society of Gene Therapy

doi:10.1016/S1525-0016(02)00034-5

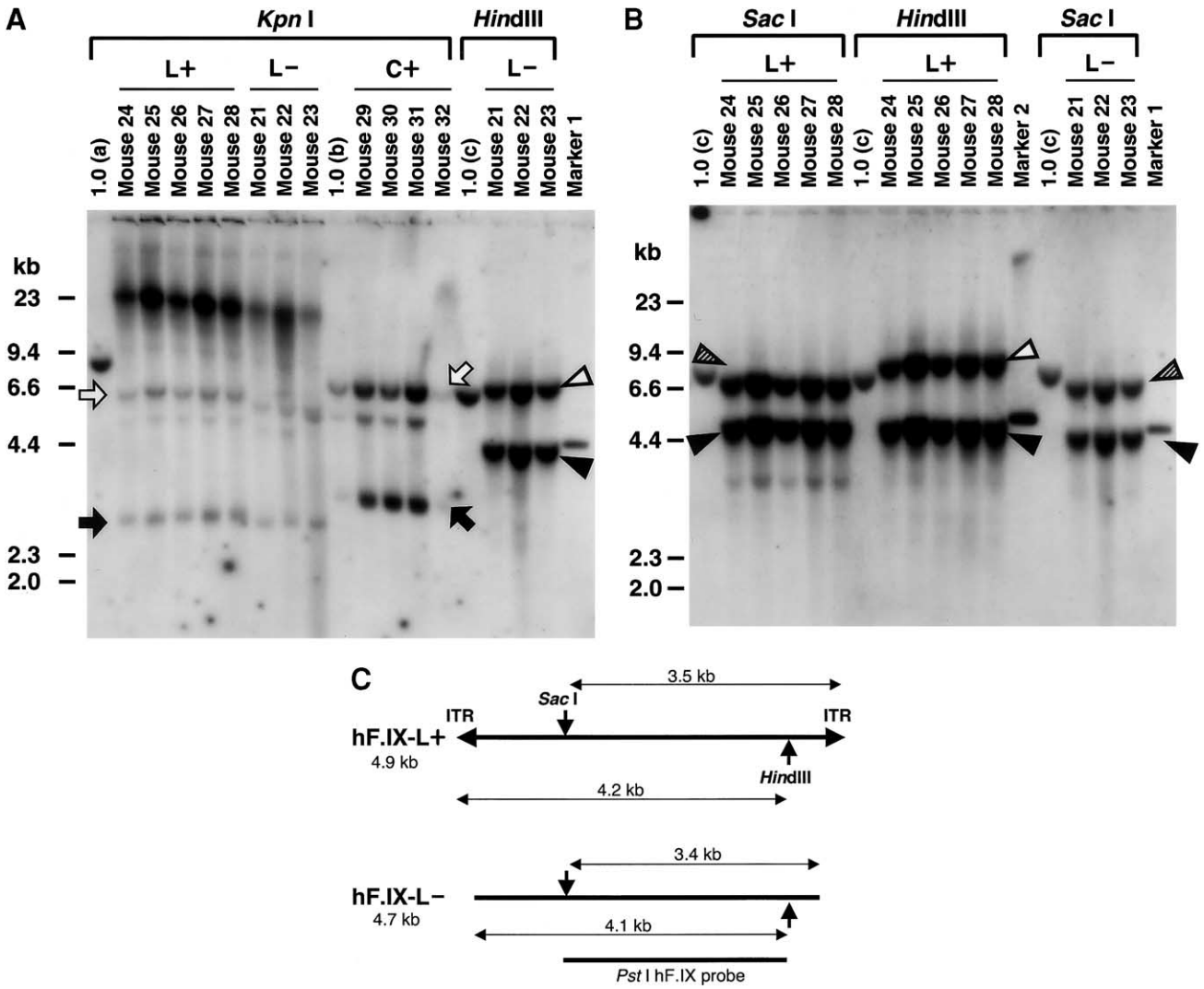

FIG. 6. Southern blot analysis of vector genomes in mouse livers transfected with hF.IX-L+, hF.IX-L−, or hF.IX-C+ molecules. (A, B) Molecular fate of hF.IX-L+, hF.IX-L−, or hF.IX-C+ molecules in mouse liver. C57BL/6 mice were injected with 22–100 μg of each molecule through the tail vein, and mouse livers were harvested 6 weeks after injection for analysis. Mice 21–23, mice 24–26, mice 27 and 28, mice 29 and 30, and mice 31 and 32 received 22 μg of hF.IX-L−, 23 μg of hF.IX-L+, 91 μg of hF.IX-L+, 25 μg of hF.IX-C+, and 100 μg of hF.IX-C+, respectively. A 20 μg sample of total DNA was digested with *Kpn*I (non-cutter for vector genomes), *Sac*I (5′ cutter) or *Hin*dIII (3′ cutter), separated on a 0.8% agarose gel, and probed with a vector sequence-specific *Pst*I human F.IX probe (*Pst*I hF.IX probe, see panel C). The lanes labeled 1.0 are copy number standards based on plasmids pV4.1e-hF.IX (a), hF.IX-C+ (b), and pVm4.1eδD-hF.IX (c). Plasmids (a) and (c) were linearized with the enzymes indicated, confirming that the digestion was complete. Marker 1, *Pvu*II-digested pBSδD-hF.IX, serving as a 1.0-unit marker for hF.IX-L−; marker 2, *Pvu*II-digested pVm4.1eδD-hF.IX, serving as a 1.0-unit marker for hF.IX-L+. Supercoiled and relaxed ds circular monomers are indicated as closed and open arrows, respectively. Head-to-tail, head-to-head, and tail-to-tail molecules are indicated as closed, open, and hatched arrowheads, respectively. The size markers are from *Hin*dIII-digested λ-DNA. (C) The restriction maps of hF.IX-L+ and hF.IX-L−.

DNA transfection. However, an alternative explanation is that the results in the study by Yang *et al.* [18] represent a time-dependent shift from linear concatemers to circular concatemers, and may not represent recombination or joining between supercoiled ds circular monomers. Recently Song *et al.* reported that ds linear rAAV vector genomes were maintained for over a year in C57BL/6 severe combined immunodeficiency (SCID) mouse muscle [23]. In their study, the lack of the DNA-dependent protein kinase catalytic subunit (DNA-PKcs) in SCID mice slowed further recombination of linear molecules. This observation suggests that ds linear molecules could be stably maintained, escaping nuclease attack in cells, and could be substrates for further genome conversion.

Two other explanations could account for the differences between our findings and those by Yang *et al.* [18].

Copyright © The American Society of Gene Therapy

First, cellular entry, nuclear trafficking, and processing of rAAV vector genomes delivered as a viral vector may be different from that of naked DNA delivered with transfection. Recombinant AAV vectors are internalized by receptor-mediated endocytosis from clathrin-coated pits [24,25], whereas cellular entry of naked DNA has not been clearly defined. A recent report has demonstrated that the fate of rAAV vector genomes is influenced by the processing pathway in endosomes, which may affect vector-mediated transgene expression [26]. Also, the cellular response to incoming ssDNA and dsDNA or vector particles might be different, and this may result in induction of different subsets of proteins involved in genome processing and conversion. In addition, we do not know whether transfected naked ds vector genomes and vector genomes delivered as a rAAV vector reside at the same location within the nuclei. Localization of vector genomes within a cell may affect transgene expression or the fate of vector genomes.

Second, in this study we used supercoiled ds circular monomers with a DDITR sequence as a representative form of ds circular rAAV vector genomes. This rationale was based on a previous study by Duan *et al*. [19] demonstrating, by chemical sequencing of ds circular rAAV vector genomes rescued in bacteria, that the predominant forms of circular monomers were circles with a DDITR sequence. However, the DDITR structure may be predominant because of selective pressure that eliminates less stable circular forms containing two joined ITR sequences in bacteria, making them undetectable by this type of assay. It remains to be elucidated whether there are other predominant forms of supercoiled ds circular rAAV vector genomes in transduced cells that undergo intermolecular recombination or joining.

We have been interested in whether or not ds circular or linear rAAV vector genomes can efficiently integrate into chromosomes *in vivo,* and a series of experiments to explore this question are ongoing. To date our results indicate that supercoiled ds circular monomers with a DDITR are not the substrates for efficient chromosome integration in hepatocytes *in vivo*. However, we cannot totally exclude the possibility of the presence of short-lived circular intermediates for integration or concatemerization, which cannot be detected by Southern blot analysis or plasmid rescue technique [21].

The human F.IX plasmids (hF.IX-C+ and hF.IX-C−) used in this study mediated persistent expression in mouse livers *in vivo,* which was unusual because most of supercoiled plasmid vectors mediate transient transgene expression *in vivo*. Until recently, it was believed that transient expression from plasmid DNA vectors was due to quick degradation of vector DNA in target tissues. However, recent studies have shown that plasmid DNA could persist in the liver, resulting in long-term high transgene expression depending on the plasmid construct [27,28]. Interestingly, when the EF1α-hF.IX cassette was incorporated into a 'sleeping beauty' transposon vector plasmid backbone and introduced into mouse liver as naked plasmid DNA, human F.IX expression was negligible within 3 weeks [15,29], whereas the same cassette within the rAAV vector plasmid backbone resulted in human F.IX expression lasting for at least 6 weeks at high levels ([14], and data not shown). Although we cannot explain these differences, it supports an earlier finding that the bacterial plasmid backbone also has a function in the persistence of transgene expression, and the effect is related to transcriptional silencing rather than vector DNA stability [22].

In summary, we used a technique to assess directly the capacity of ds linear rAAV vector genomes versus ds circular forms to concatemerize *in vivo*. We found that, contrary to an earlier finding, ds linear rAAV genomes, not circular genomes, were substrate for concatemerization. Although concerns exist as to how far our system represents rAAV- mediated gene delivery *in vivo,* these findings demonstrate that further study of the mechanisms of *in vivo* rAAV genome conversion is warranted to delineate fully the pathway from ss rAAV genome entry into the nucleus to transgene expression. Furthermore, our demonstration that free DNA ends, not AAV-ITRs, are substrates for concatemerization has important implications, not only toward our understanding of rAAV transduction, but also for many other gene transfer strategies.

Materials and Methods

Construction of plasmids. The maps of dsDNA molecules are shown in Figure 1. Construction of plasmids pDDITRAAV-EF1α-hF.IX.AO, which carries a DDITR (hF.IX-C+), and pEF1α-hF.IX.AO, a control plasmid for hF.IX-C+ that lacks a DDITR (hF.IX-C−), was as follows. pUC620, a pUC119-based plasmid containing wild-type AAV serotype 2 genome (provided by Avigen Inc.), was digested with *Acl*I to disrupt the ampicillin resistance gene (Amp^r) in the pUC119 backbone, and ligated to a *Xmn*I-*Dra*III fragment from pCR2.1 (Invitrogen, Carlsbad, CA) that contained the prokaryotic kanamycin resistance gene (Km^r), to make pUC620Km^r. The wild-type AAV-2 sequence was cut out from pUC620Km^r by *Ppu*MI and *Sna*BI double digestion, and replaced with a *Rsr*II-*Rsr*II fragment of pAAV-EF1α-nlsGFP.AOSP2 containing the elongation factor 1α enhancer-promoter (EF1αEP), the prokaryotic *lac* operon promoter, the enhanced green fluorescent protein (EGFP) gene from pEGFP (Clontech, Palo Alto, CA) with a nuclear- localizing signal, and the human β-globin polyadenylation signal (βglpA), to make pAAV-EF1α-nlsGFP.AOSP.Km^r. pAAV-EF1α-nlsGFP.AOSP2 was derived from pAAV-EF1α-GFP.AOSP [16] containing a nuclear-localizing signal from pECFP-Nuc (Clontech). pAAV-EF1α-nlsGFP.AOSP.Km^r was cut with *Msc*I to remove all the stuffer backbone together with a part of the ITR sequences, and was ligated to a 117-bp *Msc*I-*Msc*I fragment of the ITR, to make pDDITRAAV-EF1α-nlsGFP.AOP. This plasmid carried a 165-bp DDITR, short stretches of wild-type AAV-2-derived sequence flanking both edges of the DDITR, and the EF1α-nlsGFP expression cassette. These short stretches of wild-type AAV-2 sequence were essential to keep the DDITR sequence intact in *Escherichia coli,* because the DDITR sequence in plasmids was not retained when it was directly inserted into the original pAAV-EF1α-GFP.AOSP or pAAV-EF1α-nlsGFP.AOSP2 as described earlier (data not shown). To construct pDDITRAAV-EF1α-hF.IX.AO, a fragment containing the *lac* operon promoter, the nlsGFP gene, and βglpA was removed by *Eco*RI-*Aat*II double digestion and replaced with a *Eco*RI-*Bbr*II fragment of pV4.1e-hF.IX [30] containing the human F.IX (hF.IX) cDNA and the human growth hormone polyade-

Copyright © The American Society of Gene Therapy

doi:10.1016/S1525-0016(02)00034-5

nylation signal (hGHpA). The resulting plasmid, pDDITRAAV-EF1α-hF.IX.AO, contained a truncated EF1α enhancer-promoter (δEF1αEP) [16], hF.IX cDNA, hGHpA, Amp^r, and plasmid origin of replication (ori) next to the DDITR. pEF1α-hF.IX.AO was constructed from pEF1α-nlsGFP.AOP by replacing its *Eco*RI-*Alw*NI fragment containing the gene encoding GFP with an *Eco*RI-*Alw*NI fragment of pDDITRAAV-EF1α-hF.IX.AO containing the hF.IX cDNA. pEF1α-nlsGFP.AOP was made by self-ligation of a *Not*I-*Not*I fragment containing the nlsGFP expression cassette and the Amp^r-ori cassette of pAAV-EF1α-nlsGFP.AOSP2. The integrity of the DDITR sequence was confirmed by directly sequencing the plasmids or sequencing the purified *Sma*I or *Bgl*I fragments whose secondary structures on the ITR sequence were relaxed.

hF.IX-L+ and hF.IX-L− are agarose gel-purified *Pvu*II-*Pvu*II fragments of pVm4.1eδD-hF.IX [31] and pBSδD-hF.IX, respectively. *Pvu*II digestion of pVm4.1eδD-hF.IX resulted in excision of EF1αhF.IX expression cassette with two ITRs. The ITRs in hF.IX-L+ molecules were 130 bp long, shortened by 15 bp in the region A from the end of the ITR. To construct pBSδD-hF.IX, a 4.6-kb *Not*I-*Not*I fragment containing the EF1α-hF.IX expression cassette was excised from pVm4.1eδD-hF.IX, and inserted at a unique *Not*I site of a pBluescript-based shuttle plasmid, which has a *Pvu*II-*Not*I-*Pvu*II linker. From the resulting pBSδD-hF.IX, a 4.6-kb EF1α-hF.IX expression cassette could be excised by *Pvu*II digestion. All the plasmids were propagated in Dcm+ Dam+ *SURE E. coli* (Stratagene, Ceder Creek, TX) except for pV4.1e-hF.IX.dam-, which was grown in Dcm− Dam− DM1 strain of *E. coli,* and purified by one cycle of CsCl gradient ultracentrifugation. Because a considerable amount of concatenated plasmids were present in hF.IX-C+ preparations (Fig. 2), we purified supercoiled monomers by agarose gel fractionation at least once, and DNA was recovered by electroelution. Even after three cycles of gel fractionation of monomeric hF.IX-C+ molecules, we still observed high-molecular-weight plasmids, suggesting that some aggregation of monomeric hF.IX-C+ molecules occurred (Fig. 2). There was no difference in plasma human F.IX levels in animals treated with hF.IX-C+ molecules purified with one (n = 24) or three cycles (n = 13) of agarose gel fractionation (data not shown). Monomeric hF.IX-C− molecules were also purified in the same way, although we did not observe extensive concatenation or aggregation of the molecules as seen in hF.IX-C+ preparations. hF.IX-L+ and the control, hF.IX-L−, were prepared by digesting CsCl-purified pVm4.1eδD-hF.IX or pBSδD-hF.IX with *Pvu*II followed by agarose gel fractionation in the same way. All the DNA preparations were filtered through a 0.22-μm syringe filter unit before *in vivo* administration.

Animal procedures. Six- to 8-week-old female C57BL/6 mice were obtained from Jackson Laboratory (Bar Harbor, ME). All animal procedures were done according to the guidelines for animal care at Stanford University. Hydrodynamics-based *in vivo* hepatocyte transfection of naked plasmid DNA by tail vein injection, and partial hepatectomy were performed as earlier described [29,32–34]. Blood samples were collected from the retro-orbital plexus.

Measurement of human F.IX in samples. ELISA specific for human F.IX was employed for the measurement of human F.IX in mouse plasma samples using affinity-purified plasma human F.IX (Calbiochem, La Jolla, CA) as a standard [35].

Southern blot analysis. Total genomic DNA was extracted from mouse livers and subjected to Southern blot analysis as described [14,16]. The vector genome copy number standards (the number of ds vector genomes per diploid genomic equivalent) were total liver DNAs from a naive mouse mixed with the appropriate amount of control plasmid. Band intensities were quantified using a G710 Calibrated Imaging Densitometer (Bio-Rad, Hercules, CA). Replication of vector genomes was detected on the basis of loss of *Dpn*I sensitivity, as described in detail elsewhere [14]. Integrated vector genomes lose methylation at adenine residues in *Dpn*I recognition sites when hepatocytes pass through S-phase twice or more after a two-thirds partial hepatectomy, and become *Dpn*I resistant.

ACKNOWLEDGMENTS

We thank Clare E. Thomas for critical reading of this manuscript. This work was supported by NIH grant HL64274.

RECEIVED FOR PUBLICATION NOVEMBER 12, 2001; ACCEPTED NOVEMBER 13, 2002.

REFERENCES

1. Nakai, H., Storm, T. A., and Kay, M. A. (2000). Increasing the size of rAAV-mediated expression cassettes *in vivo* by intermolecular joining of two complementary vectors. *Nat. Biotechnol.* **18:** 527–532.
2. Duan, D., Yue, Y., Yan, Z., and Engelhardt, J. F. (2000). A new dual-vector approach to enhance recombinant adeno-associated virus-mediated gene expression through intermolecular *cis* activation. *Nat. Med.* **6:** 595–598.
3. Sun, L., Li, J., and Xiao, X. (2000). Overcoming adeno-associated virus vector size limitation through viral DNA heterodimerization. *Nat. Med.* **6:** 599–602.
4. Girod, A., *et al. (1999). Genetic capsid modifications allow efficient re-targeting of adeno-associated virus type 2. Nat. Med.* **5:** 1052–1056.
5. Davidson, B. L., *et al. (2000). Recombinant adeno-associated virus type 2, 4, and 5 vectors: transduction of variant cell types and regions in the mammalian central nervous system. Proc. Natl. Acad. Sci. USA* **97:** 3428–3432.
6. Chao, H. E., *et al.* (2000). Several log increase in therapeutic transgene delivery by distinct adeno-associated viral serotype vectors. *Mol. Ther.* **2:** 619–623, doi: 10.1006/mthe.2000.0207.
7. Xiao, W., *et al.* (1999). Gene therapy vectors based on adeno-associated virus type 1. *J. Virol.* **73:** 3994–4003.
8. McCarty, D. M., Monahan, P. E., and Samulski, R. J. (2001). Self-complementary recombinant adeno-associated virus (scAAV) vectors promote efficient transduction independently of DNA synthesis. *Gene Ther.* **8:** 1248–1254.
9. Wagner, J. A., *et al.* (1999). Safety and biological efficacy of an adeno-associated virus vector-cystic fibrosis transmembrane regulator (AAV-CFTR) in the cystic fibrosis maxillary sinus. *Laryngoscope* **109:** 266–274.
10. Stedman, H., Wilson, J. M., Finke, R., Kleckner, A. L., and Mendell, J. (2000). Phase I clinical trial utilizing gene therapy for limb girdle muscular dystrophy: α-, β-, γ-, or Δ-sarcoglycan gene delivered with intramuscular instillations of adeno-associated vectors. *Hum. Gene Ther.* **11:** 777–790.
11. Kay, M. A., *et al.* (2000). Evidence for gene transfer and expression of Factor IX in haemophilia B patients treated with an AAV vector. *Nat. Genet.* **24:** 257–261.
12. Miao, C. H., *et al.* (1998). The kinetics of rAAV integration in the liver. *Nat. Genet.* **19:** 13–15.
13. Miao, C. H., *et al.* (2000). Nonrandom transduction of recombinant adeno-associated virus vectors in mouse hepatocytes *in vivo*: cell cycling does not influence hepatocyte transduction. *J. Virol.* **74:** 3793–3803.
14. Nakai, H., Storm, T. A., and Kay, M. A. (2000). Recruitment of single-stranded recombinant adeno-associated virus vector genomes and intermolecular recombination are responsible for stable transduction of liver *in vivo. J. Virol.* **74:** 9451–9463.
15. Nakai, H., *et al.* (2001). Extrachromosomal recombinant adeno-associated virus vector genomes are primarily responsible for stable liver transduction *in vivo. J. Virol.* **75:** 6969–6976.
16. Nakai, H., Iwaki, Y., Kay, M. A., and Couto, L. B. (1999). Isolation of recombinant adeno-associated virus vector-cellular DNA junctions from mouse liver. *J. Virol.* **73:** 5438–5447.
17. Chen, S. J., Tazelaar, J., Moscioni, A. D., and Wilson, J. M. (2000). *In vivo* selection of hepatocytes transduced with adeno-associated viral vectors. *Mol. Ther.* **1:** 414–422, doi: 10.1006/mthe.2000.0065.
18. Yang, J., *et al.* (1999). Concatamerization of adeno-associated virus circular genomes occurs through intermolecular recombination. *J. Virol.* **73:** 9468–9477.
19. Duan, D., Yan, Z., Yue, Y., and Engelhardt, J. F. (1999). Structural analysis of adeno-associated virus transduction circular intermediates. *Virology* **261:** 8–14.
20. Xiao, X., Xiao, W., Li, J., and Samulski, R. J. (1997). A novel 165-base-pair terminal repeat sequence is the sole *cis* requirement for the adeno-associated virus life cycle. *J. Virol.* **71:** 941–948.
21. Duan, D., *et al.* (1998). Circular intermediates of recombinant adeno-associated virus have defined structural characteristics responsible for long-term episomal persistence in muscle tissue. *J. Virol.* **72:** 8568–8577.
22. Chen, Z. Y., *et al.* (2001). Linear DNAs concatemerize *in vivo* and result in sustained transgene expression in mouse liver. *Mol. Ther.* **3:** 403–410, doi: 10.1006/mthe.2001.0278.
23. Song, S., Laipis, P. J., Berns, K. I., and Flotte, T. R. (2001). Effect of DNA-dependent protein kinase on the molecular fate of the rAAV2 genome in skeletal muscle. *Proc. Natl. Acad. Sci. USA* **98:** 4084–4088.
24. Duan, D., *et al.* (1999). Dynamin is required for recombinant adeno-associated virus type 2 infection. *J. Virol.* **73:** 10371–10376.
25. Bartlett, J. S., Wilcher, R., and Samulski, R. J. (2000). Infectious entry pathway of adeno-associated virus and adeno-associated virus vectors. *J. Virol.* **74:** 2777–2785.

Copyright © The American Society of Gene Therapy

26. Duan, D., Yue, Y., Yan, Z., Yang, J., and Engelhardt, J. F. (2000). Endosomal processing limits gene transfer to polarized airway epithelia by adeno-associated virus. *J. Clin. Invest.* **105:** 1573–1587.
27. Miao, C. H., Thompson, A. R., Loeb, K., and Ye, X. (2001). Long-term and therapeutic-level hepatic gene expression of human Factor IX after naked plasmid transfer *in vivo*. *Mol. Ther.* **3:** 947–957, doi: 10.1006/mthe.2001.0333.
28. Zhang, G., Song, Y. K., and Liu, D. (2000). Long-term expression of human α1-antitrypsin gene in mouse liver achieved by intravenous administration of plasmid DNA using a hydrodynamics-based procedure. *Gene Ther.* **7:** 1344–1349.
29. Yant, S. R., *et al.* (2000). Somatic integration and long-term transgene expression in normal and haemophilic mice using a DNA transposon system. *Nat. Genet.* **25:** 35–41.
30. Nakai, H., *et al.* (1998). Adeno-associated viral vector-mediated gene transfer of human blood coagulation Factor IX into mouse liver. *Blood* **91:** 4600–4607.
31. Burton, M., *et al.* (1999). Coexpression of Factor VIII heavy and light chain adeno-associated viral vectors produces biologically active protein. *Proc. Natl. Acad. Sci. USA* **96:** 12725–12730.
32. Kay, M. A., *et al.* (1992). Hepatic gene therapy: persistent expression of human α1-antitrypsin in mice after direct gene delivery *in vivo*. *Hum. Gene Ther.* **3:** 641–647.
33. Liu, F., Song, Y., and Liu, D. (1999). Hydrodynamics-based transfection in animals by systemic administration of plasmid DNA. *Gene Ther.* **6:** 1258–1266.
34. Zhang, G., Budker, V., and Wolff, J. A. (1999). High levels of foreign gene expression in hepatocytes after tail vein injections of naked plasmid DNA. *Hum. Gene Ther.* **10:** 1735–1737.
35. Walter, J., You, Q., Hagstrom, J. N., Sands, M., and High, K. A. (1996). Successful expression of human Factor IX following repeat administration of adenoviral vector in mice. *Proc. Natl. Acad. Sci. USA* **93:** 3056–3061.

Copyright © The American Society of Gene Therapy